



Thermodynamics of AdS black holes from deflection angle formalism

A. Belhaj ^{a,*}, H. Belmahi ^a, M. Benali ^a, A. Segui ^{b,1}

^a Département de physique, Équipe des Sciences de la matière et du rayonnement, ESMAr, Faculté des Sciences, Université Mohammed V de Rabat, Rabat, Morocco

^b Departamento de física teórica, Universidad de Zaragoza, E-50009 Zaragoza, Spain



ARTICLE INFO

Article history:

Received 8 March 2021

Accepted 19 April 2021

Available online 27 April 2021

Editor: N. Lambert

Keywords:

AdS black holes

Thermodynamics

Deflection angle of lights

ABSTRACT

We explore a link between AdS black hole thermodynamics and the deflection angle variation. Using the elliptic function analysis, we first study the phase structure of RN-AdS solutions in terms of optical aspects. Precisely, we find that the stable and the unstable phases can be derived from thermal variations of the deflection angle. Then, we investigate the Hawking-Page transition from the Gibbs energy optical dependence. Among others, we reveal that the large black hole/small black hole transition occurs at a specific value of the deflection angle. The finding results, being confirmed by the help of the Ruppeiner metric of the phase state space, indicate that the deflection angle can be exploited to unveil data on thermodynamics of AdS black holes.

© 2021 The Author(s). Published by Elsevier B.V. This is an open access article under the CC BY license (<http://creativecommons.org/licenses/by/4.0/>). Funded by SCOAP³.

Contents

1. Introduction	1
2. Deflection angle of RN-AdS black holes	2
3. Stability of RN-AdS black holes vs the deflection angle	3
4. Deflection angle and Hawking-Page phase transition	4
5. Geothermodynamics and the deflection angle	5
6. Conclusions and final remarks	7
Declaration of competing interest	7
Acknowledgements	7
References	7

1. Introduction

Recently, black holes have been considered as a central subject in modern physics, being supported by the recent observations associated with the Event Horizon Telescope (EHT) providing a direct imaging of a black hole at the center of M87 galaxy [1–3] and gravitational wave detections [4]. Precisely, this investigation direction has attracted huge attentions in connection with other topics dealing with classical and quantum gravity models. Various aspects of such fascinating objects have been studied by examining the asso-

ciated thermodynamical and optical behaviors. For thermodynamic properties, black holes in the Anti-de-Sitter space (AdS) with a negative cosmological constant Λ have been approached using different analytical and numerical ways and methods. Interpreting Λ as a pressure p , these black holes exhibit similarities with results dealing with generic fluids [5–11]. A special emphasis has been put on the case of Reissner-Nordstrom Anti-de-sitter black hole (RN-AdS) in four dimensions. Precisely, it has been revealed that the associated physics shares similar pictures as the Van der Waal fluids [12]. Moreover, many behaviors associated with the Gibbs free energy G and phase transitions have been treated showing non-trivial results corresponding to the second order phase transition between large black holes (LBH) and small black holes (SBH), the existence of a minimal temperature (T_0) and the Hawking Page transition at temperature (T_{HP}). The letter reveals a transition between a LBH and a thermal AdS background required by $G = 0$.

* Corresponding author.

E-mail addresses: a-belhaj@um5r.ac.ma (A. Belhaj), hajar_belmahi@um5.ac.ma (H. Belmahi), mohamed_benali4@um5.ac.ma (M. Benali), segui@unizar.es (A. Segui).

¹ Authors in alphabetical order.

Concerning optical aspects, the geometrical shadows and the deflection angle of certain black holes have been investigated [13–18]. Concretely, shadows of non-rotating black holes involve perfect circular geometries where the involved size can depend on some parameters including the mass and the charge. It has been shown, however, that the rotating parameter distorts such a circular picture providing deformed configurations with D-shapes [19]. These optical behaviors can be approached using astronomical observables controlling the size and the shape of the shadows. Taking appropriate values, the shadows of Kerr solutions could provide relevant results compared with EHT collaborations [20]. Moreover, the deflection angle of lights has been also studied using different roads and methods. Gibbons and Werner suggested a direct way to compute such a quantity using the Gauss-Bonnet theorem applied to a spacial background described by the optic metric [21]. Alternatively, it has been proposed a method using the elliptic integral formalism. It has been given an explicit solution in terms of Weierstrass elliptic functional forms [22,23]. In particular, complete and incomplete elliptic functions have also been exploited to express the deflection angle [24,25].

More recently, thermodynamical properties of RN-AdS black holes and shadow aspects have been combined. In particular, it has been shown that one can approach black hole thermodynamics from shadow behaviors [26,27]. Concretely, it has been remarked that such aspects can be exploited to establish a link between shadows and critical properties. A close inspection reveals that the deflection angle could depend on certain thermodynamical quantities. This observation has been inspired by considering two RN-AdS black holes with two different temperatures and the same impact factor. At this level, one could naturally ask questions concerning the deflection angle variation in the thermodynamical systems.

The aim of this work is to explore an alternative way of approaching thermodynamics of AdS black holes using a deflection angle formalism. For RN-AdS black holes in four dimensions, we show that this optical quantity allows one to unveil data on thermodynamical behaviors. Concretely, we establish an interplay between the RN-AdS black hole thermodynamics and the deflection angle variation. Preforming elliptic function analysis, we first approach the phase structure of such black holes from the deflection thermal variation. Then, we investigate the Hawking-Page transition from the Gibbs energy optical dependence. Among others, we show that the LBH/SBH transition occurs at a specific value of the deflection angle. This transition takes the same place for generic values of the impact parameter b . The obtained findings, supported by the Ruppeiner metric of the phase state space, explore that the deflection angle could be suggest to provide data on the AdS black hole thermodynamics.

The organization of this work is as follows. In section 2, we reconsider the deflection angle study of the RN-AdS black holes in four dimensions. In section 3, we investigate the phase structure by varying the deflection angle. In section 4, we reconsider the study of the Hawking-Page (HP) transition in terms of the deflection angle variation. In section 5, we implement the optical behaviors in the phase state space using the Ruppeiner metric computations. The last section is devoted to conclusions and final remarks.

2. Deflection angle of RN-AdS black holes

In this section, we re-examine the behavior of the deflection angle of AdS black holes in four dimensions which will be exploited to approach stability aspects and phase transitions. For simplicity reasons, we deal with RN-AdS black holes [28,29]. The corresponding action is given by

$$S = \frac{1}{16\pi} \int \sqrt{-g} dx^4 \left(R - F^{\mu\nu} F_{\mu\nu} + \frac{6}{\ell^2} \right). \quad (2.1)$$

In this action, R represents the Ricci scalar curvature. $F_{\mu\nu} = \partial_\mu A_\nu - \partial_\nu A_\mu$ is the Maxwell tensor, where A is the electromagnetic potential vector. ℓ denotes the AdS radius being related to a negative cosmological constant Λ via the relation $\Lambda = -\frac{3}{\ell^2}$. In the Boyer-Lindquist coordinates, the solution of the equations of motion, corresponding to the above action, can be expressed as

$$ds^2 = g_{\mu\nu} dx^\mu dx^\nu = -f(r) dt^2 + \frac{dr^2}{f(r)} + r^2(d\theta^2 + \sin^2\theta d\phi^2), \quad (2.2)$$

where the metric function $f(r)$ reads as follows

$$f(r) = 1 - \frac{2M}{r} + \frac{Q^2}{r^2} + \frac{r^2}{\ell^2}. \quad (2.3)$$

It is noted that M and Q represent the mass and the charge, respectively. In this way, the potential 1-form defined by $F = dA$ takes the following form

$$A_\mu = \left(-\frac{Q}{r}, 0, 0, 0 \right). \quad (2.4)$$

Using the event horizon radius r_h , being the largest real root of the metric function f , and laws of thermodynamics, we can compute the relevant quantities. In particular, the mass, the temperature and the entropy are given by the following relations

$$M = \frac{r_h^4 + \ell^2 r_h^2 + \ell^2 Q^2}{2\ell^2 r_h}, \quad (2.5)$$

$$T = \frac{3r_h^4 + \ell^2(r_h^2 - Q^2)}{4\pi\ell^2 r_h^3}, \quad (2.6)$$

$$S = \pi r_h^2. \quad (2.7)$$

In the equatorial plane $\theta = \frac{\pi}{2}$, the Euler-Lagrange equations for null geodesics provide the following equations of motion

$$\dot{\phi} = \frac{L}{r^2}, \quad (2.8)$$

$$\dot{r}^2 = E^2 - f(r) \frac{L^2}{r^2}, \quad (2.9)$$

where L and E are conserved quantities corresponding to the energy and the angular momentum, respectively. Implementing, the impact parameter $b = \frac{L}{E}$, the equation (2.9) becomes

$$\dot{r}^2 = E^2 \left(1 - \frac{f(r)}{r^2} b^2 \right). \quad (2.10)$$

In what follows, we consider a light ray starting from the infinity. Then, it approaches to the black hole until the distance of closest approach r_0 , and then it goes back to infinity. In this case, the ray is in the deflection angle zone and the impact parameter is constrained by $b > b_0$, where b_0 is the critical value for which the photons can perform an unstable circular orbit around a black hole. The critical value r_0 can be obtained from the following conditions

$$V_{eff}(r) |_{r=r_0} = 0, \quad \frac{dV_{eff}(r)}{dr} |_{r=r_0} = 0, \quad (2.11)$$

where V_{eff} is the effective potential taking the form

$$V_{eff}(r) = E^2 \left(\frac{f(r)}{r^2} b^2 - 1 \right). \quad (2.12)$$

Exploiting (2.11) and (2.12), one gets

$$r_0 = \frac{3M + \sqrt{9M^2 - 8Q^2}}{2}. \quad (2.13)$$

Putting r_0 in the effective potential equation, we obtain the critical value $b_0 = \sqrt{\frac{r_0^2}{f(r_0)}}$. To express the deflection angle Θ , one needs the total change in ϕ which is given by $2|\phi(r_0) - \phi(\infty)|$. Assuming that the trajectory is a straight line, the change in ϕ equals to π . Indeed, this gives

$$\begin{aligned} \Theta &= 2|\phi(r_0) - \phi(\infty)| - \pi, \\ &= 2 \int_{r_0}^{\infty} \left| \frac{d\phi}{dr} \right| dr - \pi. \end{aligned} \quad (2.14)$$

Combining the equations (2.8) and (2.9), one finds

$$\left(\frac{d\phi}{dr} \right)^2 = \frac{A^2}{P(r)}, \quad (2.15)$$

where $\frac{1}{A^2} = \frac{1}{b^2} - \frac{1}{\ell^2}$ and $P(r) = r^4 - A^2(r^2 - 2Mr + Q^2)$. It is noted that $P(r)$ involves four real roots indicated by $r_1 < r_2 < r_3 < r_4$. The largest root defines the critical value r_0 . Performing the following variable redefinitions $u = r - r_0$, ϕ becomes a function of u

$$\phi(u) = \int_0^u \frac{Adu}{\sqrt{u(u+u_1)(u+u_2)(u+u_3)}}, \quad (2.16)$$

where $u_1 = r_0 - r_1$, $u_2 = r_0 - r_2$, $u_3 = r_0 - r_3$. The integral of the equation (2.16) can be calculated either in terms of the first kind of complete and incomplete elliptic functions or the Weierstrass elliptic functions. Adopting the second method and according to [22], one can redefine the equation (2.16) as follows

$$\phi(x) = \lambda \int_x^{\infty} \frac{dx}{\sqrt{4x^3 - g_2x - g_3}}. \quad (2.17)$$

Taking the following changes $\alpha = u_1^{-1} + u_2^{-1} + u_3^{-1}$, $\beta = (u_1u_2)^{-1} + (u_3u_1)^{-1} + (u_3u_2)^{-1}$, $\gamma = (u_1u_2u_3)^{-1}$, $\lambda = \frac{A}{\sqrt{u_1u_2u_3}}$, $x = \frac{1}{4u} + \frac{\alpha}{12}$ in the equation (2.16), the expressions of the arguments g_2 and g_3 take the forms

$$g_2 = \frac{1}{4} \left(\frac{\alpha^2}{3} - \beta \right), \quad g_3 = \frac{1}{16} \left(\frac{\alpha\beta}{3} - \gamma - \frac{2\alpha^3}{27} \right). \quad (2.18)$$

Solving the equation (2.17) in terms of the Weierstrass elliptic function $x = \wp(\frac{\phi}{\lambda}, g_2, g_3)$, we can get the expression of the function $\phi(r)$ which reads as

$$\phi(r) = \lambda \wp^{-1} \left(\frac{1}{r - r_0} + \frac{\alpha}{12}, g_2, g_3 \right). \quad (2.19)$$

Considering the equations (2.14) and (2.19), we can obtain the deflection angle of the RN-AdS black hole. It is given by

$$\Theta = 2|\lambda \wp^{-1} \left(\frac{\alpha}{12}, g_2, g_3 \right)| - \pi. \quad (2.20)$$

A close inspection reveals that the optical quantity Θ is controlled by four parameters (b, ℓ, Q, M) defining the associated black hole moduli space. Fixing the values of the mass and the AdS radius, the variation of the deflection angle as a function of the impact parameter for several values of Q is plotted in Fig. 1. Indeed, this figure represents the expected behavior of the deflection angle as a continuous function of the impact parameter. It has been observed that this optical angle decreases when the charge increases. Similar optical aspects have been remarked for various AdS black holes [30,31]. Having discussed optical behaviors of RN-AdS black holes, we move to approach the associated thermodynamics properties using the deflection angle variation.

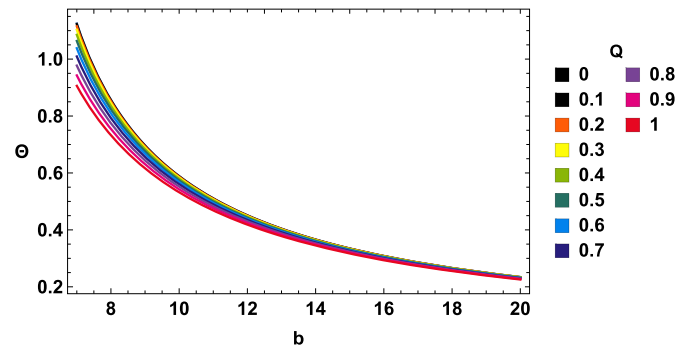


Fig. 1. Variation of the deflection angle in terms of the impact parameter for different values of the charge by taking $\ell = 172$, $M = 1$.

3. Stability of RN-AdS black holes vs the deflection angle

In this section, we investigate the charged black hole stability using optical aspects. In particular, we show that the stability requirement can be approached in terms of the deflection angle. To make a connection between the conditions under which a black hole is stable and such an optical quantity, we exploit the sign of the heat capacity, being a relevant thermodynamical quantity in the stability analysis. It is recalled that the condition $C = T \left(\frac{\partial S}{\partial T} \right) > 0$ defines the stable phase and the unstable one corresponds to $C = T \left(\frac{\partial S}{\partial T} \right) < 0$. To implement the deflection angle, we extend the heat capacity expression as follows

$$C = T \left(\frac{\partial S}{\partial r_h} \right) \left(\frac{\partial r_h}{\partial \Theta} \right) \left(\frac{\partial \Theta}{\partial T} \right). \quad (3.1)$$

Taking into account the constraint $\frac{\partial S}{\partial r_h} > 0$, the crucial information on the stability phase can be encoded in the sign of the product $\left(\frac{\partial r_h}{\partial \Theta} \right) \left(\frac{\partial \Theta}{\partial T} \right)$. To handle such a product, we first re-examine the temperature behaviors in terms of r_h in different regions of the black hole moduli space. This is needed to inspect the involved phase structures [26]. Precisely, the obtained data will be examined by exploring the deflection angle variation. Fixing the value of the AdS radius via the relation $\ell^2 = \frac{675}{4\pi}$ and using the equation (2.6), Fig. 2 illustrates the temperature as a function of the event horizon radius r_h for various values of the charge. For charge values in the range $0.1 \leq Q \leq 1$, the temperature behaviors are presented in dotted, dashed, and solid curves. It follows from this figure that the stable states of the black hole correspond to the dotted and the solid curves, where the temperature is an increasing function of r_h . However, the dashed curves are associated with the unstable phase. Therefore, the phase structure of the RN-AdS black holes can be approached from the quantity $\frac{dT}{dr_h}$. To understand how the deflection angle can reflect the phase structure, we consider the variation of Θ in terms of r_h . This is plotted in Fig. 3. For generic regions of the black hole moduli space, it has been remarked that the deflection angle is a decreasing function of r_h , without any critical value. It provides a continuous function for the variable r_h . In this way, the information about the phase structures can be extracted from the sign of the quantity $\frac{dT}{d\Theta}$. Concretely, the stable and the unstable phases correspond, respectively, to the following constraints

$$\frac{dT}{d\Theta} < 0, \quad \frac{dT}{d\Theta} > 0. \quad (3.2)$$

To investigate the interplay between the phase transitions and the deflection angle, we exploit the temperature expression given in the equation (2.6). Indeed, such thermal behaviors are depicted in

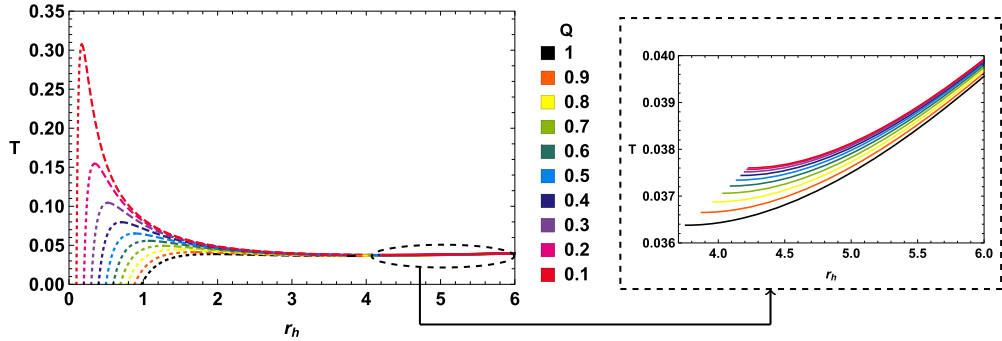


Fig. 2. Variation of the temperature in terms of the horizon radius for $\ell^2 = \frac{675}{4\pi}$.

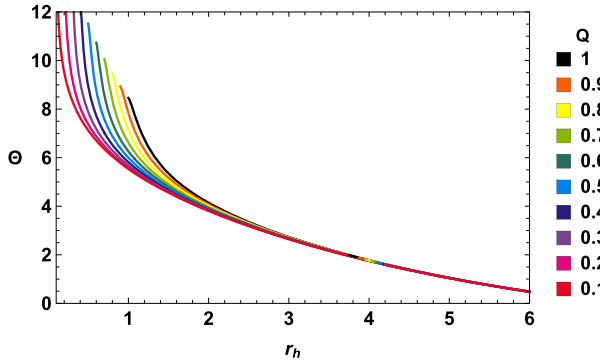


Fig. 3. Variation of the deflection angle in terms of r_h for different values of the charges by taking $b = 10$ and $\ell^2 = \frac{675}{4\pi}$.

Fig. 4, by taking into account the previous regions of the stable and the unstable phases associated with r_h . Effectively, the stable and the unstable phases are manifested in such a figure. These behaviors, which match perfectly with results presented in Fig. 2, show that the phase structure can be investigated from using the optical aspects relying on the deflection angle variation. Following the heat capacity of the RN-AdS black hole, the sign changing at critical points can be investigated in terms of the temperature dependence of the deflection angle. Indeed, for a stable phase, the deflection angle is a decreasing function of the temperature. This phase is represented by solid and dotted curves. For the unstable one, however, the deflection angle increases with the temperature. This is represented by dashed curves. The present findings could suggest that such a deflection angle can be considered as a new tool for studying phase transitions of charged AdS black holes from optical aspect.

4. Deflection angle and Hawking-Page phase transition

In this section, we explore the relation between the deflection angle and the Hawking-page transition of RN-AdS black holes in four dimensions. It is noted that the Gibbs free energy is the relevant thermodynamical quantity providing physical data to investigate such a transition [7,32]. Taking RN-AdS black holes in a grand canonical ensemble, with a fixed electric potential Φ , this quantity reads as

$$G = M - TS - \Phi Q, \quad (4.1)$$

where Φ is the electric potential given by $\Phi = \frac{Q}{r_h}$. Interpreting the cosmological constant as a pressure via the relation $p = \frac{3}{8\pi\ell^2}$, and using the electric potential, calculations give the following needed relations

$$T = \frac{8\pi pr_h^2 - \Phi^2 + 1}{4\pi r_h}, \quad (4.2)$$

$$M = \frac{r_h(8\pi pr_h^2 + 3\Phi^2 + 3)}{6}, \quad (4.3)$$

being obtained from the previous quantities. Substituting (4.2), (4.3) into (4.1), one obtains the Gibbs free energy, as a function of r_h , p and Φ ,

$$G = \frac{(3r_h - 8\pi pr_h^3 - 3r_h\Phi^2)}{12}. \quad (4.4)$$

An examination on the temperature function $T = T(r_h, p, \Phi)$ shows that the RN-AdS black hole possesses two critical values.

The first one associated with the critical value $T_0 = \sqrt{\frac{2p(1-\Phi^2)}{\pi}}$ corresponds to the minimum of this function, below which no black hole can survive [33]. Solving the horizon radius r_h in terms of the temperature T , we get two solutions associated with large and small black holes relying on two different even horizon radius r_h^+ and r_h^- , respectively. Presenting in the Fig. 5 the event horizon radius as a function of the temperature for different values of charge and a fixed value of the pressure $p = 0.04$, such a critical value is indicated by the intersection of the LBH, represented by dashed curves, and the SBH solid curves. The second relevant critical value $T_{HP} = \sqrt{\frac{8p(1-\Phi^2)}{3\pi}}$ is the point where the Hawking-Page transition takes place, a situation which both the radiation and the black hole have a vanishing Gibbs free energy. To illustrate graphically the associated behaviors, the variation of the Gibbs free energy in terms of the temperature for LBH and SBH is plotted in Fig. 6.

Effectively, the Hawking-Page behaviors and the minimum temperature are presented in this figure. To make a contact with the optical quantities, we first replace the event horizon radius in the expression of the deflection angle by the temperature. Then, we inspect the variation of the deflection angle function $\Theta = \Theta(b, T, p, \Phi)$ with respect to T and b . For fixed values of Φ and p , a 3-dimensional behavior is illustrated in Fig. 7. It has been observed a minimum temperature which does not depend on the b direction of the associated moduli space. For $b > r_h^0$, where r_h^0 is associated with T_0 , the variation of the impact parameter b does not affect the black hole temperature. This can be understood from the intrinsic behaviors of black holes.

Looking for the Hawking-Page transition from optical aspects of the charged black holes, we consider the variation of the Gibbs free energy in terms of the deflection angle. The behavior is presented in Fig. 8. For LBH, we get a vanishing Gibbs free energy corresponding to $\Theta = \Theta_c$. This imitates the Hawking-page transition behavior where this critical value could play the same role as $r_h = r_{HP}$ for which $T = T_{HP}$. It has been remarked that LBH is manifested when G is an increasing function of Θ . However, SBH appears when G decreases with such a quantity. As expected, the

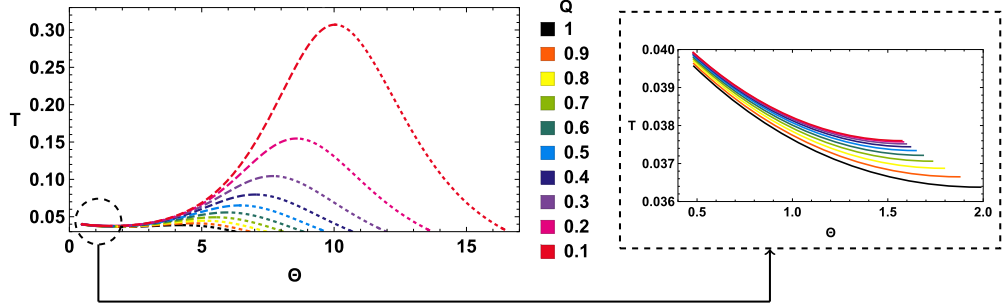


Fig. 4. Variation of the temperature in terms of the deflection angle for $b = 10$ and $\ell^2 = \frac{675}{4\pi}$.

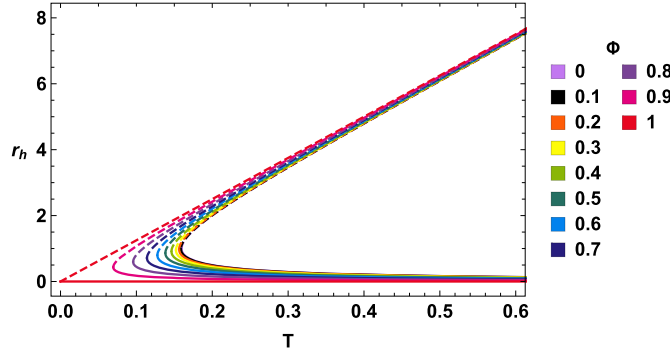


Fig. 5. Variation of the event horizon radius in terms of the temperature.

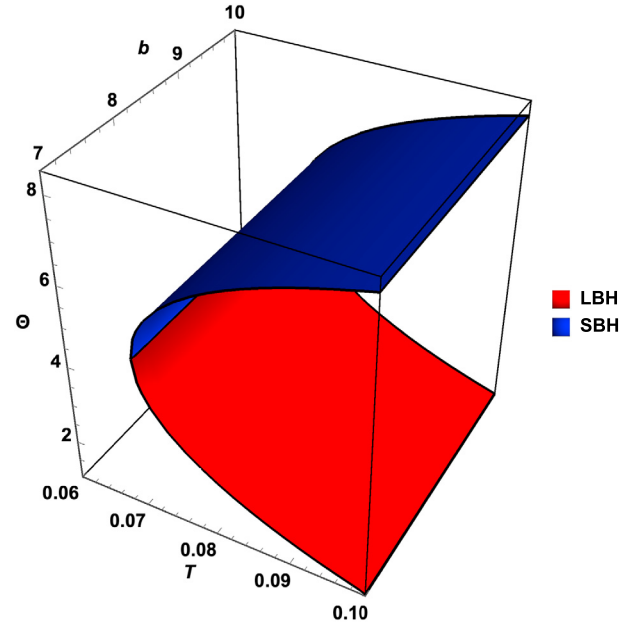


Fig. 6. Behavior of the Gibbs free energy as function of the temperature for $\Phi = 0.9$ and $p = 0.04$.

intersection point of LBH and SBH which corresponds to a minimum temperature value provides a maximum value of the Gibbs free energy at a critical value $\Theta = \Theta_0$. This result could confirm the previous finding which reveals that the deflection angle can be exploited as a relevant quantity to approach critical behaviors of charged AdS black holes in four dimensions.

5. Geothermodynamics and the deflection angle

In this section, we implement the deflection angle in the investigation of the AdS black hole thermodynamics from geometric properties of the phase state space. It is noted that the associated data are encoded in a thermodynamic potential Ψ and conserved quantities considered as space coordinates denoted usually by x_i [34]. In this way, the involved metric takes the following form

$$g_{ij} = \frac{\partial^2 \Psi}{\partial x_i \partial x_j}. \quad (5.1)$$

It is recalled, in passing, that Ψ shares similarities with the Kähler potential explored in the metric building of complex manifolds in-

Fig. 7. Gibbs free energy in terms of the temperature and the impact parameter b for $p = 0.04$ and $\Phi = 0.9$.

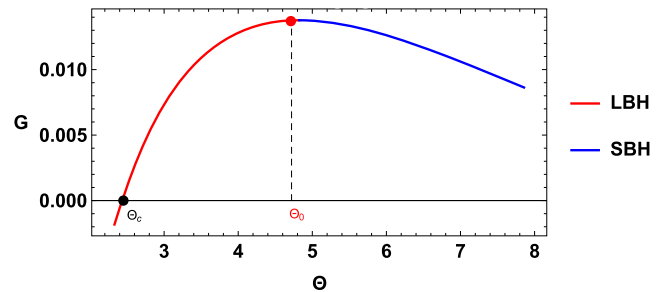


Fig. 8. Variation of the Gibbs free energy in function of Θ for $\Phi = 0.9$ and $p = 0.04$.

cluding Calabi-Yau geometries [35]. Many metric forms have been elaborated to unveil information on critical behaviors of black hole objects. More details can be found in [34,36]. For simplicity reasons, we consider the Ruppeiner metric where the thermodynamic potential Ψ is identified with the entropy function S [37]. Taking a two dimensional geometry, for the RN-AdS black hole, the metric (5.1) reduces to

$$g_{ij} = -\frac{\partial S}{\partial x_i \partial x_j}, \quad i, j = 1, 2. \quad (5.2)$$

Using $x_1 = M$ and $x_2 = Q$, the metric (5.2) can be written as

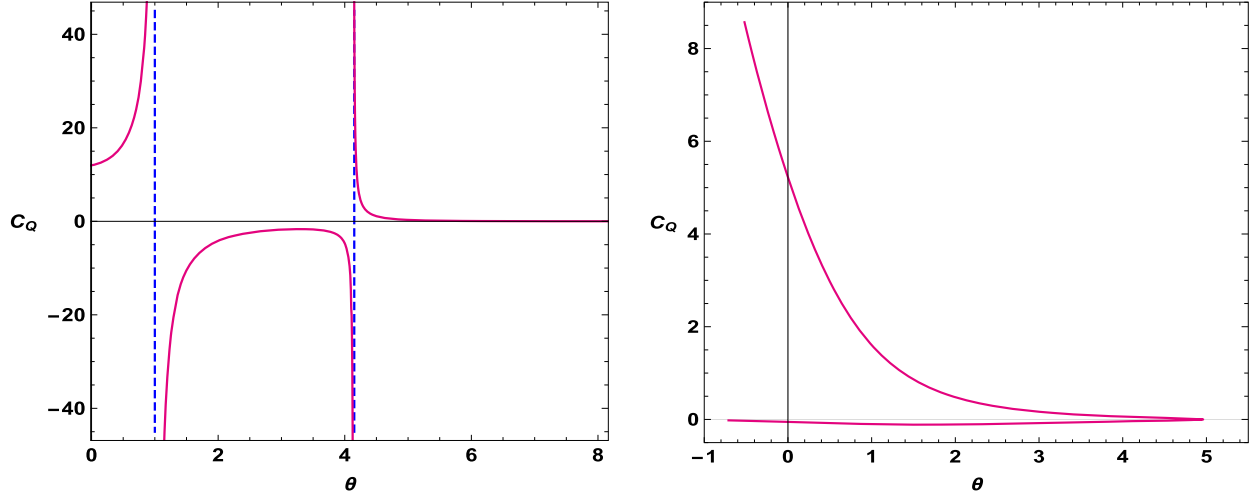


Fig. 9. Variation of the heat capacity in terms of Θ . Left: $Q = 0.11$. Right: $Q = 0.5$.

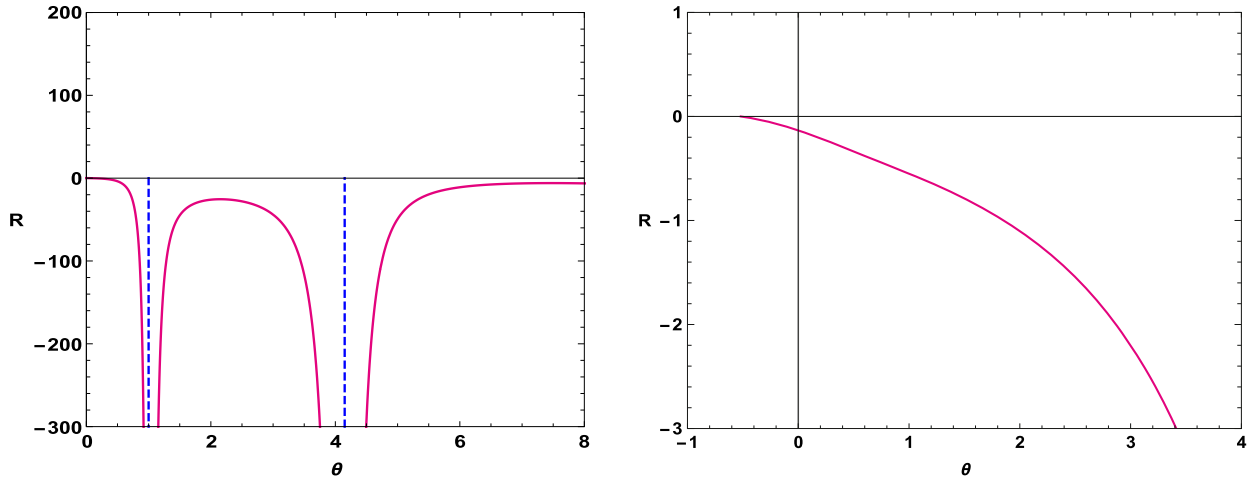


Fig. 10. Variation of the Ruppeiner invariant R in terms of Θ . Left: $Q = 0.11$. Right: $Q = 0.5$.

$$g_{ij} = \begin{pmatrix} -\frac{\partial S(M, Q)}{\partial M^2} & -\frac{\partial S(M, Q)}{\partial M \partial Q} \\ -\frac{\partial S(M, Q)}{\partial M \partial Q} & -\frac{\partial S(M, Q)}{\partial Q^2} \end{pmatrix}. \quad (5.3)$$

According to [38], the curvature scalar R , which encodes data on critical behaviors, reads as

$$R = -\frac{18r^6(3Q^2 - r^2) + 3\ell^2r^2(10Q^4 - 9Q^2r^2 + 3r^4) + \ell^4(Q^2 - r^2)^2}{\pi\ell^4(3r^4/\ell^2 - Q^2 + r^2)(3r^4/\ell^2 + 3Q^2 - r^2)^2}. \quad (5.4)$$

This geometric quantity can share the same divergence behaviors provided by the heat capacity in terms either of the event horizon or the entropy. This analysis of the phase transition using such a geometric method has been extensively investigated showing a nice interplay between thermodynamics and Riemannian geometries [36]. Motivated by such activities, we numerically discuss such aspects from the deflection angle formalism. In this way, the expression of the heat capacity, at constant charges, will be needed. Indeed, it is given by

$$C_Q = T \left(\frac{\partial S}{\partial T} \right)_Q = \frac{2\pi r^2(\ell^2(r^2 - Q^2) + 3r^4)}{\ell^2(3Q^2 - r^2) + 3r^4}. \quad (5.5)$$

It has been revealed that the phase transition LBH/SBH occurs at a range of charge values Q bounded by a critical value Q_c , where

one has $Q < Q_c$. For a sake of simplicity, we consider particular regions of the moduli space. Taking $\ell = 1$, for instance, this critical value has been found to be $Q_c = 0.408$. Plugging the deflection angle in the equation (5.5), we plot the variation of the heat capacity, at constant charges, as a function of Θ in the left and the right of Fig. 9 for $Q < Q_c$ and $Q > Q_c$, respectively. For $Q < Q_c$, the phase transition behavior is manifested, where we have a discontinuous curve for the singular points $\Theta_1 \simeq 1.01$ and $\Theta_2 \simeq 4.15$, illustrated by blue dashed lines. For $Q > Q_c$, however, a continuous curve with non divergence behaviors is observed, which indicates that there is only one black hole solution.

Consider now the curvature scalar behavior. Fixing the value of the impact parameter $b = 10$, we examine the variation of R in terms of Θ for the above charge conditions $Q < Q_c$ and $Q > Q_c$. Such behaviors are depicted in Fig. 10. For $Q < Q_c$, it has been observed that R is a discontinuous function of Θ , which exhibits similar divergent points appearing in the heat capacity variation. For $Q > Q_c$, however, R is a continuous function without singular locations, matching with the heat capacity aspects. As expected, the deflection angle can be considered as a relevant parameter providing data on black hole thermodynamical properties. This confirms the results obtained in the previous sections. We anticipate to note that such an optical quantity could be exploited as a tool to reflect curved features on the phase state space. This non-trivial remark deserves more investigations. We hope to address such a question in future works.

6. Conclusions and final remarks

In this work, we have explored a relation between RN-AdS black hole thermodynamics in four dimensions and the deflection angle variation. In particular, we have examined how this optical quantity can reflect some thermodynamical behaviors of such black holes. Firstly, we have exploited the Weierstrass elliptic function to reconsider the deflection angle expression. Then, we have established a connection between the phase structure of RN-AdS solutions and the deflection angle dependence. The stability depends on the thermal variation of such an angle. Concretely, we have found that the stable phase is associated with decreasing behaviors. However, the unstable one corresponds to increasing behaviors.

To support the present finding, we have approached the Hawking-Page transition from the Gibbs free energy optical variation. Precisely, we have shown that the LBH/SBH transition occurs at a specific value of the deflection angle. It has been remarked that such a transition takes the same place for generic values of the impact parameter.

The obtained results have been confirmed by the help of geometric properties of the phase state space with the Ruppeiner metric. It has been observed that geometric properties of such a space could be controlled by the deflection angle variations. This has suggested that the deflection angle can be exploited to unveil data on thermodynamics of the charged AdS black holes.

This work comes up with certain open questions. It should be interesting to consider others parameters and backgrounds either in four dimensions or in arbitrary dimensions. These investigations could open new windows to deal with black hole thermodynamics using the phase state space controlled by the deflection angle variations. These questions could be addressed in future works.

Declaration of competing interest

The authors declare that they have no known competing financial interests or personal relationships that could have appeared to influence the work reported in this paper.

Acknowledgements

The authors would like to thank A. El Balali, W. El Hadri, H. El Moumni, Y. Hassouni, E. Torrente-Lujan, and M. B. Sedra for collaborations and discussions on related topics. This work is partially supported by the ICTP through AF-13. The work of AS is funded by Ministerio de Economía y Competitividad under Grant No. FPA2015-65745-P (MINECO/FEDER) and DGA-FSE grant 2020-E21-17R.

References

- [1] K. Akiyama, et al., First M87 Event Horizon Telescope results. IV. Imaging the central supermassive black hole, *Astrophys. J.* **L4** (1) (2019) 875, arXiv:1906.11241.
- [2] K. Akiyama, et al., First M87 Event Horizon Telescope results. V. Imaging the central supermassive black hole, *Astrophys. J.* **L5** (1) (2019) 875.
- [3] K. Akiyama, et al., First M87 Event Horizon Telescope results. VI. Imaging the central supermassive black hole, *Astrophys. J.* **L6** (1) (2019) 875.
- [4] B. Abbott, et al., Observation of gravitational waves from a binary black hole merger, *Phys. Rev. Lett.* **116** (6) (2016) 061102, arXiv:1602.03837.
- [5] J.D. Bekenstein, Black holes and entropy, *Phys. Rev. D* **7** (8) (1973) 2333.
- [6] S.W. Hawking, Black holes and thermodynamics, *Phys. Rev. D* **7** (2) (1976) 191.
- [7] S.W. Hawking, D.N. Page, Thermodynamics of black holes in anti-de Sitter space, *Commun. Math. Phys.* **87** (4) (1983) 577.
- [8] A. Belhaj, M. Chabab, H. El Moumni, M.B. Sedra, On thermodynamics of AdS black holes in arbitrary dimensions, *Curr. Psychol. Lett.* **29** (2012) 100401, arXiv:1210.4617.
- [9] Y. Liu, D.C. Zou, B. Wang, Signature of the Van der Waals like small-large charged AdS black hole phase transition in quasinormal modes, *J. High Energy Phys.* **09** (2014) 179, arXiv:1405.2644.
- [10] A. Belhaj, M. Chabab, H. El Moumni, K. Masmar, M.B. Sedra, A. Segui, On heat properties of AdS black holes in higher dimensions, *J. High Energy Phys.* **05** (2015) 149, arXiv:1503.07308.
- [11] A. Belhaj, A. El Balali, W. El Hadri, E. Torrente-Lujan, On universal constants of AdS black holes from Hawking-page phase transition, *Phys. Lett. B* **811** (2020) 135871, arXiv:2010.07837.
- [12] A. Rajagopal, D. Kubiznak, R.B. Mann, Van der Waals black hole, *Phys. Lett. B* **737** (2014) 277, arXiv:1408.1105.
- [13] A. Övgün, I. Sakalli, J. Saavedra, Shadow cast and deflection angle of Kerr-Newman-Kasuya spacetime, *J. Cosmol. Astropart. Phys.* **10** (2018) 041, arXiv:1807.00388.
- [14] A. Belhaj, H. Belmahi, M. Benali, W. El Hadri, H. El Moumni, E. Torrente-Lujan, Shadows of 5D black holes from string theory, *Phys. Lett. B* **812** (2021) 136025, arXiv:2008.13478.
- [15] R. Konoplya, Shadow of a black hole surrounded by dark matter, *Phys. Lett. B* **795** (2019) 1, arXiv:1905.00064.
- [16] A. Grenzebach, V. Perlick, C. Lämmerzahl, Photon regions and shadows of Kerr-Newman-NUT black holes with a cosmological constant, *Phys. Rev. D* **89** (12) (2014) 124004, arXiv:1403.5234.
- [17] S. Haroon, M. Jamil, K. Jusufi, K. Lin, R.B. Mann, Shadow and deflection angle of rotating black holes in perfect fluid dark matter with a cosmological constant, *Phys. Rev. D* **99** (12) (2019) 044015, arXiv:1810.04103.
- [18] A. Grenzebach, V. Perlick, C. Lämmerzahl, Photon regions and shadows of accelerated black holes, *Int. J. Mod. Phys. D* **24** (09) (2015) 1542024, arXiv:1503.03036.
- [19] S.U. Khan, J. Ren, Shadow cast by a rotating charged black hole in quintessential dark energy, *Phys. Dark Universe* **30** (2020) 100644, arXiv:2006.11289.
- [20] S.W. Wei, Y.C. Zou, Y.X. Liu, R.B. Mann, Curvature radius and Kerr black hole shadow, *J. Cosmol. Astropart. Phys.* **08** (2019) 030, arXiv:1904.07710.
- [21] G.W. Gibbons, M.C. Werner, Applications of the Gauss-Bonnet theorem to gravitational lensing, *Class. Quantum Gravity* **25** (23) (2008) 235009, arXiv:0807.0854.
- [22] J.R. Villanueva, J. Saavedra, M. Olivares, N. Cruz, Photons motion in charged Anti-de Sitter black holes, *Astrophys. Space Sci.* **344** (2) (2013) 437.
- [23] G.W. Gibbons, M. Vyska, The application of Weierstrass elliptic functions to Schwarzschild null geodesics, *Class. Quantum Gravity* **29** (2012) 065016, arXiv:1110.6508.
- [24] R. Uniyal, H. Nandan, P. Jetzer, Bending angle of light in equatorial plane of Kerr-Sen black hole, *Phys. Lett. B* **782** (2018) 185, arXiv:1803.04268.
- [25] P. Sharma, H. Nandan, R. Gannouji, R. Uniyal, A. Abebe, Deflection of light by a rotating black hole surrounded by quintessence, *Int. J. Mod. Phys. A* **35** (2020) 2050155, arXiv:1911.00372.
- [26] M. Zhang, M. Guo, Can shadows reflect phase structures of black holes?, *Eur. Phys. J. C* **80** (2020) 790, arXiv:1909.07033.
- [27] A. Belhaj, L. Chakchhi, H. El Moumni, J. Khaloufi, K. Masmar, Thermal image and phase transitions of charged AdS black holes using shadow analysis, *Int. J. Mod. Phys. A* **35** (27) (2020) 2050170, arXiv:2005.05893.
- [28] L.J. Romans, Supersymmetric, cold and lukewarm black holes in cosmological Einstein-Maxwell theory, *Nucl. Phys. B* **383** (1992) 395, arXiv:hep-th/9203018.
- [29] L.A.J. London, Arbitrary dimensional cosmological multi-black holes, *Nucl. Phys. B* **434** (1995) 709.
- [30] W. Javed, J. Abbas, A. Övgün, Effect of the quintessential dark energy on weak deflection angle by Kerr Newmann black hole, *Ann. Phys.* **418** (2020) 168183, arXiv:2007.16027.
- [31] A. Belhaj, M. Benali, A. El Balali, H. El Moumni, S-E. Ennafi, Deflection angle and shadow behaviors of quintessential black holes in arbitrary dimensions, *Class. Quantum Gravity* **37** (2020) 215004, arXiv:2006.01078.
- [32] D. Kubiznak, R.B. Mann, M. Teo, Black hole chemistry: thermodynamics with Lambda, *Class. Quantum Gravity* **34** (2017) 063001, arXiv:1608.06147.
- [33] Y-Y. Wang, B-Y. Su, N. Li, Hawking Page phase transitions in four-dimensional Einstein Gauss Bonnet gravity, *Phys. Dark Universe* **31** (2021) 100769, arXiv:2008.01985.
- [34] F. Weinhold, Metric geometry of equilibrium thermodynamics, *J. Chem. Phys.* **63** (1975) 2479.
- [35] B.R. Greene, String theory on Calabi-Yau manifolds, arXiv:hep-th/9702155.
- [36] H. Quevedo, A. Sanchez, S. Taj, A. Vazquez, Phase transitions in geometrothermodynamics, *Gen. Relativ. Gravit.* **43** (2011) 1153, arXiv:1010.5599.
- [37] G. Ruppeiner, Riemannian geometry in thermodynamic fluctuation theory, *Rev. Mod. Phys.* **67** (1995) 605.
- [38] P. Wang, H. Wu, H. Yang, Thermodynamic geometry of AdS black holes and black holes in a cavity, *Eur. Phys. J. C* **80** (2020) 216, arXiv:1910.07874.